MATHEMATICAL MODEL AND EXPERIMENTAL STUDY OF THE STARTUP REGIMES OF UNCONTROLLED AND GAS-CONTROLLED LOW-TEMPERATURE HEAT PIPES

V. V. Barsukov, V. I. Demidyuk, and G. F. Smirnov

UDC 536.58

A mathematical model of the startup regimes of uncontrolled and gas-controlled heat pipes is developed, and the results of experiments are given. The experimental data are compared with the calculations.

Transient operating regimes play an important part in the operation of systems using low-temperature heat pipes. Only limited experimental work has been done on these regimes [1, 2], and recommendations for the calculation of their dynamic characteristics are virtually nonexistent. In the present article we describe investigations (analytical and experimental) of the startup regimes of uncontrolled* and gas-controlled heat pipes from a state with a molten heat-transfer medium.

For the development of a mathematical model of the heat-pipe startup regimes we use the familiar method of modelling of operating regimes of heat-engineering systems whereby the elements of the system are characterized as lumped-parameter objects [3]. We adopt the following assumptions.

1. The following can be disregarded because of their small contributions: a) heat transfer via structural elements of the heat pipe in the axial direction; b) thermal resistance at phase interfaces; c) the quantity of energy necessary to raise the pressure in the vapor passage of the heat pipe; d) the transport time of vapor from the heat-input section to the condenser section.

2. The values of the thermal resistance between elements of the thermal model of the heat pipe are constant.

*Hereinafter we drop the term "uncontrolled."

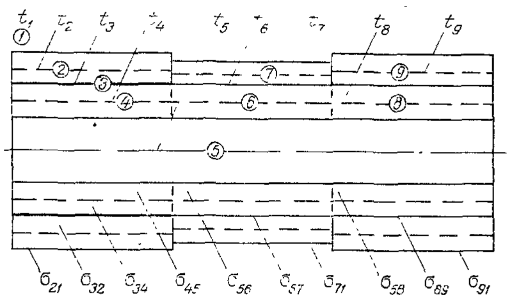

Fig. 1. Thermal model of the heat pipe (t_i = mean temperature of i-th element; σ_{ij} = thermal conductance between midsections of i-th and j-th elements). 1) Surrounding medium; 2, 7) thermal insulation; 3) heat source; 4, 6, 8) walls with capillary structure along evaporator, transport, and condenser sections, respectively; 5) vapor-flow passage; 9) heat-rejection zone.

Odessa Technological Institute of the Refrigeration Industry. Translated from Inzhenerno-Fizicheskii Zhurnal, Vol. 35, No. 3, pp. 389-396, September, 1978. Original article submitted October 24, 1977.

0022-0841/78/3503-1011$07.50

TABLE 1. Scheme of Computation of Coefficients σ_{ij} for Heat-Pipe (HP) Model

Thermal conductance	Heat-transfer mechanism	Analytical relations: plane HP	Analytical relations: cylindrical HP
σ_{32}	Heat conduction	$\sigma_{32}=2\lambda_2 S_2/\delta_2$	$\sigma_{32}=\dfrac{4\pi\lambda_2 l_2}{\ln(d_2'/d_2'')}$
σ_{21}	Combination heat conduction, convection, and radiation	$\sigma_{21}=1\Big/\left(\dfrac{1}{K_{1E}S_{1E}}+\dfrac{1}{\sigma_{32}}\right)$; $K_{1E}=\alpha_{rE}+\alpha_{cE}$	
σ_{34}	Heat conduction	$\sigma_{34}=2\lambda_4 S_4/\delta_4$	$\sigma_{34}=\dfrac{4\pi\lambda_4 l_4}{\ln(d_4'/d_4'')}$
σ_{45}	Heat conduction	$\sigma_{45}=\sigma_{34}$	
σ_{56}	Heat conduction	$\sigma_{56}=2\lambda_6 S_6/\delta_6$	$\sigma_{56}=\dfrac{4\pi\lambda_6 l_6}{\ln(d_6'/d_6'')}$
σ_{58}	Heat conduction	$\sigma_{58}=2\lambda_8 S_8/\delta_8$	$\sigma_{58}=\dfrac{4\pi\lambda_8 l_8}{\ln(d_8'/d_8'')}$
σ_{67}	Heat conduction through multilayer wall	$\sigma_{67}=\dfrac{2S_6}{\sum_{i=6}^{7}\delta_i/\lambda_i}$	$\sigma_{67}=\dfrac{4\pi l_6}{\sum_{i=6}^{7}\dfrac{\ln(d_i'/d_i'')}{\lambda_i}}$
σ_{71}	Combination heat conduction, convection, and radiation	$\sigma_{71}=1\Big/\left(\dfrac{1}{K_{1T}S_{1T}}+\dfrac{1}{K_{2T}}\right)$; $K_{1T}=\alpha_{rT}+\alpha_{cT}$	
		$K_{2T}=2\lambda_7 S_7/\delta_7$	$K_{2T}=\dfrac{4\pi\lambda_7 l_7}{\ln(d_7'/d_7'')}$
	Heat conduction through multilayer wall (contact cooling)	$\sigma_{89}=\dfrac{2S_8}{\sum_{i=8}^{9}\delta_i/\lambda_i}$	$\sigma_{89}=\dfrac{4\pi l_8}{\sum_{i=8}^{9}\dfrac{\ln(d_i'/d_i'')}{\lambda_i}}$
σ_{89}	Combination heat conduction, convection, and radiation (Convective cooling)	$\sigma_{89}=1\Big/\left(\dfrac{1}{K_9 S_9}+\dfrac{1}{\sigma_{58}}\right)$; $K_9=\alpha_r+\alpha_c$	
σ_{91}	Combination heat conduction, convection, and radiation	$\sigma_{91}=1\Big/\left(\dfrac{1}{K_{1C}S_{1C}}+\dfrac{1}{K_{2C}}\right)$; $K_{1C}=\alpha_{rC}+\alpha_{cC}$	
		$K_{2C}=2\lambda_9 S_9/\delta_9$	$K_{2C}=\dfrac{4\pi\lambda_9 l_9}{\ln(d_9'/d_9'')}$

The thermal model of the heat pipe for our calculations is illustrated in Fig. 1. The mathematical model is conceived as a system of equations of energy conservation (heat balance) written for the i-th element of the thermal model. The heat-balance equation for the i-th element has the general form

$$C_i\,\frac{d\vartheta_i}{d\tau}+\sum_{j=1}\sigma_{ij}(\vartheta_i-\vartheta_j)=N_i\,. \qquad (1)$$

Here $C_i=\sum_{k=1}^{m}V_{ik}\rho_{ik}c_{ik}$; V_{ik}, ρ_{ik}, c_{ik} are the volume, density, and specific heat of the k-th component of the i-th heat-pipe element (m = 1 for homogeneous elements).

The thermal conductances σ_{ij} between lumped-parameter cross sections of the i-th and j-th elements are determined according to the recommendations of [4]. As an illustration, Table 1 gives the scheme of computation of the coefficient σ_{ij} for the postulated thermal model (without regard for phase-transition thermal resistance).

It is important to note that in special cases certain elements of the postulated thermal model, such as the insulation along individual sections, can be omitted, thereby decreasing the number of equations in the system. Equation (1) is reduced to the standard form

$$\frac{d\vartheta_i}{d\tau}+\sum_{j=1}^{n} a_{ij}\vartheta_j = A_i\,, \tag{2}$$

where

$$a_{ij} = -\sigma_{ij}/C_i;\ a_{ii} = \sum_{j=1}^{n} \sigma_{ij}/C_i;\ A_i = N_i/C_i\,. \tag{3}$$

Under the stated assumptions for the thermal model in Fig. 1 the system of equations (1) takes the form

$$\begin{aligned}
N &= C_3\,\frac{dt_3}{d\tau} + \sigma_{32}(t_3 - t_2) + \sigma_{34}(t_3 - t_4),\\
\sigma_{32}(t_3 - t_2) &= C_2\,\frac{dt_2}{d\tau} + \sigma_{21}(t_2 - t_1),\\
\sigma_{34}(t_3 - t_4) &= C_4\,\frac{dt_4}{d\tau} + \sigma_{45}(t_4 - t_5),\\
\sigma_{45}(t_4 - t_5) &= \sigma_{56}(t_5 - t_6) + \sigma_{58}(t_5 - t_8),\\
\sigma_{56}(t_5 - t_6) &= C_6\,\frac{dt_6}{d\tau} + \sigma_{67}(t_6 - t_7),\\
\sigma_{67}(t_6 - t_7) &= C_7\,\frac{dt_7}{d\tau} + \sigma_{71}(t_7 - t_1),\\
\sigma_{58}(t_5 - t_8) &= C_8\,\frac{dt_8}{d\tau} + \sigma_{89}(t_8 - t_9),\\
\sigma_{89}(t_8 - t_9) &= C_9\,\frac{dt_9}{d\tau} + \sigma_{91}(t_9 - t_1).
\end{aligned} \tag{4}$$

Equations (4) form the initial system for calculation of the heat-pipe startup regimes. An appropriate set of initial conditions is

$$\tau = 0\ :\ t_i = t_{i0}\,. \tag{5}$$

It must be emphasized that the indicated approach enables us to take into account the phase-transition thermal resistance (corresponding to correction of the parameters σ_{45}, σ_{56}, and σ_{58}) and the energy necessary to increase the pressure in the vapor passage of the heat pipe [by the addition of a term of the form $\Delta i S_V l d\rho(T_5)/d\tau$ to the fourth equation of the system (4)]. Moreover, the thermal conductances σ_{ij} of the elements of the thermal model can be specified as variable parameters. Thus, within the framework of the postulated mathematical model of the heat-pipe startup regimes we can reject assumptions 1b, 1c, and 2. A solution of (4) as a system of first-order linear differential equations with constant coefficients can be obtained in analytical form. However, for a large number of elements n the analytical expressions are cumbersome, and the determination of the roots of the characteristic equation of order n requires recourse to numerical computations, thereby relinquishing the prime advantage of analytical solution. Hence, the startup regimes of specific heat pipes (on the basis of the postulated model) must be calculated with computer assistance. It is essential to note that the use of a computer permits the implementation of calculations according to the thermal model with variable thermal resistances.

In elementary situations (as, for example, when the heat-pipe insulation is absent and heating of the condenser section is negligible) or under additional assumptions (for example, that the mean temperature of the heat pipe is equal to the saturation temperature or that heat losses are absent in the transport section) the system of equations (4) for a constant temperature of the heat-rejection zone is reducible to the equation

$$t_3 = A_1 t_1 + A_9 t_9 + B_1 N\,[1 - B_2 \exp(-B_3\tau)], \tag{6}$$

in which A_i and B_i are constant coefficients depending on the thermal resistance and heat capacity of the elements of the thermal model.

Expression (6) permits considerable simplification of the analysis of the heat-pipe startup regimes.

The postulated mathematical model and preliminary experimental investigations provide the basis for modeling of more complex startup regimes, in particular, the startup regimes of gas-controlled heat pipes (GCHPs). A distinctive attribute of the GCHP is the presence of uncondensed impurities in the vapor passage in the inoperative state and the formation of a vapor–gas front, which blocks part of the heat conduit during operation. Clearly, during startup of a GCHP, a vapor–gas front is formed in the vicinity of the boundary between the transport and condenser sections (since intense radial vapor removal is realized only in the condenser section) and then moves to a position corresponding to the steady state. On the basis of this consideration the following assumptions are added to the previous set (exclusive of 1c and 2) in developing the mathematical of GCHP regimes:

1. The uncondensed gas obeys ideal-gas laws.

2. A conditional interface exists between the vapor and vapor–gas mixture.

3. In startup of the GCHP a boundary forms between the transport and condenser sections and then moves to a position corresponding to the steady state.

In accordance with the foregoing additional assumptions the system of equations (4) reduces to the form

$$\begin{aligned}
N &= C_3 \frac{dt_3}{d\tau} + \sigma_{32}(t_3 - t_2) + \sigma_{34}(t_3 - t_4),\\
\sigma_{32}(t_3 - t_2) &= C_2 \frac{dt_2}{d\tau} + \sigma_{21}(t_2 - t_1),\\
\sigma_{34}(t_3 - t_4) &= C_4 \frac{dt_4}{d\tau} + \sigma_{45}(t_4 - t_5),\\
\sigma_{45}(t_4 - t_5) &= \Delta i S_V\left(l \frac{d\rho}{d\tau} + \rho \frac{dl}{d\tau}\right) + \sigma_{56}(t_5 - t_6) + \sigma_{58}^*(t_5 - t_8),\\
\sigma_{56}(t_5 - t_6) &= C_6 \frac{dt_6}{d\tau} + \sigma_{67}(t_6 - t_7),\\
\sigma_{67}(t_6 - t_7) &= C_7 \frac{dt_7}{d\tau} + \sigma_{71}(t_7 - t_1),\\
\sigma_{58}^*(t_5 - t_8) &= C_8^* \frac{dt_8}{d\tau} + \sigma_{89}^*(t_8 - t_9),\\
\sigma_{89}^*(t_8 - t_9) &= C_9^* \frac{dt_9}{d\tau} + \sigma_{91}^*(t_9 - t_1),
\end{aligned} \qquad (7)$$

where

$$\sigma_{ij}^* = \frac{\sigma_{ij}}{l_C}\,[l - (l_E + l_T)];\quad C_i^* = \frac{C_i}{l_C}\,[l - (l_E + l_T)].$$

Equations (7) do not form a closed system. Invoking the Clausius–Clapeyron equation, a suitable (say, linear) approximation of the elastically curve for the particular heat-transfer medium, and the ideal-gas equation of state for the uncondensed gas, we establish the functional relations

$$\rho = BT_5/\Delta i, \qquad (8)$$

$$l = l'_{HP}\left(1 - \frac{P_0}{A + BT_5}\right)^{\dagger}, \qquad (9)$$

in which $l'_{HP} = l_{HP} + V_R/S_V$.

The system of equations (7), augmented with relations (8) and (9), represents a mathematical model of the GCHP startup regimes.† The calculations based on this model must be carried out in two stages. In the first stage (formation of the vapor–gas front) the condenser section is completely blocked:

*Equation (9) is valid after formation of the vapor–gas front. Prior to that event $l = l_E + l_T$.
†To impart generality to all the equations it is advisable to use the absolute temperature T (°K) of the elements of the thermal model.

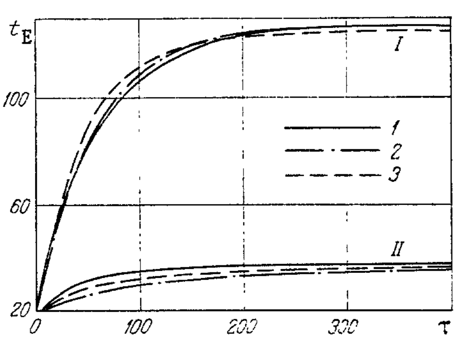

Fig. 2

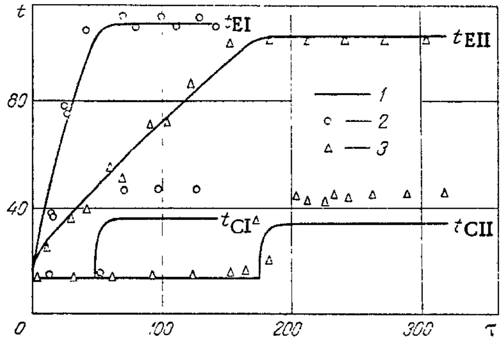

Fig. 3

Fig. 2. Curves of $t_E = f(\tau)$ for an uncontrolled heat pipe. I) Water-heat-transfer medium, N = 350 W; II) F-113 refrigerant heat-transfer medium, N = 60 W, 1) calculated according to (4); 2) according to (6); 3) experimental data; t_E in °C; τ in sec.

Fig. 3. Curves of $t_i = f(\tau)$ for a gas-controlled heat pipe, water heat pipe, water heat-transfer medium. 1) N = 350 W; II) N = 100 W; 1) calculated according to (7)-(9); 2) experimental data for N = 350 W; 3) the same for N = 100 W.

I. $0 < \tau \le \tau_1$: $l = l_E + l_T$; $\tau = 0$: $T_i = T_{i0}$; $\tau = \tau_1$: $T_5 = (1/B)[(l_{HP}P_0/[l'_{HP} - (l_E + l_T)]) - A]$.

In the second stage (propagation of vapor–gas front) heat transfer in all sections of the GCHP is taken into account:

II. $\tau_1 < \tau$: $l = l_{HP}(1 - P_0/A + BT_5)$; $\tau = \tau_1$: $T_j = T_{j0}$ $(j \ge 8)$, along with the results of solution of the first stage: $dT_i/d\tau = 0$ for $\tau \to \infty$.

In calculating the startup regimes of a GCHP with a variable-volume reservoir it is necessary to augment the mathematical model with the relation $l'_{HP} = f(T_5)$ for $\tau \ge \tau_1$. A special case of variable-volume reservoir is the sylphon bellows. Here the indicated relation is governed by the elastic properties of the sylphon bellows, the geometry of the structure, and the approximation used for the elasticity curve of the given heat-transfer medium. For a linear approximation we have the relation

$$l'_{HP} = l_{HP} + \left[l_{RO} + S_e \frac{n}{c}(A + BT_5 - P_0)\right] S_{av}/S_V.$$

To test the mathematical model we conducted experiments and calculations of the startup regimes of a heat pipe and a GCHP for the following characteristics of the test objects: length of evaporator section $l_E = 0.2$ m; length of transport section $l_T = 0.175$ m; length of condenser section $l_C = 0.1$ m; shell diameter $d_{sh} = (18 \times 1) \cdot 10^{-3}$ m; shell material, copper; diameter of capillary structure $d_W = (16 \times 2) \cdot 10^{-3}$ m; material of capillary structure, brass; mesh size of capillary structure $a = 2.37 \cdot 10^{-4}$ m; filament diameter of capillary structure $d_f = 1.24 \cdot 10^{-4}$ m; porosity of capillary structure $\varepsilon = 0.716$; heat-transfer medium, water or Freon F-113; volume of reservoir for uncondensed gas $V = 6.96 \cdot 10^{-4}$ m^3; uncondensed gas, air.

For the calculations the thermal conductances σ_{ij} and heat capacities C_i of the elements of the thermal model for the experimental object were assumed to be constant and for the most part were determined analytically with the use of tabulated data [5]. The thermal conductances of elements with a capillary structure were an exception, being determined on the basis of steady-state experimental data. The systems of differential equations (4) and (7) were solved on a Razdan-2 digital computer by the Runge–Kutta method in the Merson modification. The experiments were conducted on a test facility a diagram of which is given in [6]. The test stand was equipped with a PSR1-01 self-writing recorder, an ÉPP-09M3 automatic electronic potentiometer, and a VAS 600/300 rectifier unit. The VAS 600/300 had to be used to decrease the thickness and, hence, the heat capacity of the electrical insulation in the heat-input zone and to preclude the possible influence of the alternating-electromagnetic field on the ÉPP-09M3 potentiometer readings. The experimental results, processed in the form $t_E = f(\tau)$ and $t_C = f(\tau)$, are given in Figs. 2 and 3.* (The experimental startup curves for the heat

*Curves II in Fig. 2 represent the results for an experimental heat pipe with asbestos insulation (0.075 m in diameter) in the evaporator section. In all other cases the insulation was absent.

pipe were recorded by the PSR1-01 self-writing recorder and those for the GCHP by the ÉPP-09M3 automatic potentiometer.)

In the startup of a heat pipe with a water heat-transfer medium (curves I in Fig. 2) there is clearly uncondensed gas present in the experimental object, as evinced by the relatively steep climb of the experimental curve and the high steady-state level of t_E.

The discrepancy between the calculated and experimental values of t_C in Fig. 3 are attributable to the fact that the calculations were carried out for the mean temperatures of the sections, whereas the temperatures in the condenser section during the GCHP transient process were recorded from the readings of thermocouples situated at a distance of 20 mm from the boundary with the transport section. Nonetheless, the local experimental values obtained for $t_C = f(\tau)$ illustrate the fact that the temperature of the condenser section is constant for a certain time and then climbs abruptly, confirming the hypothesis of the formation of a vapor–gas front in the GCHP at the boundary between the transport and condenser sections. The steeper growth of the calculated temperature of the condenser section is elicited by the neglect of axial heat conduction in the structure in the calculations.

On the whole, the comparison of the calculated and experimental data leads to the conclusion that the postulated mathematical model can be used for calculation of the transient operating regimes, startup in particular, of heat pipes and GCHPs. Calculations based on the indicated model are best carried out with the aid of a computer in general. It must be emphasized that the assumption of a negligible contribution of axial heat conduction in the structure induces a certain error in the calculations. That error increases with the axial conductivity of the shell and capillary structure of the heat pipe. An analytical relation of the type (6) can be derived (for an uncontrolled heat resistance of the shell and capillary structure in the axial direction (in this case the derivation of the equation involves the mean temperature of the heat pipe, i.e., instant heating of the entire heat pipe is postulated). Consequently, under certain conditions (for example, a thick-walled copper shell) calculation of the heat-pipe startup regime according to Eq. (6) can yield a more accurate result.

It does not appear possible at the present time to ascertain more specifically the limits of application of the two proposed versions of the mathematical model, because to do so requires either a more rigorous statement of the problem, which presents patent difficulties, or the accumulation of a vast quantity of experimental data (over a wide range of variation of the parameters), which are not available to the authors at this time.

Our analysis of the startup characteristics of heat pipes and GCHPs leads to the conclusion that the pressence of uncondensed gas promotes faster heating of the active length of the heat pipe.

NOTATION

N is the power;
T, t are the temperatures;
ϑ is the excess temperature;
τ is the time;
σ is the thermal conductance;
C is the total heat capacity;
λ is the thermal conductivity;
α is the heat-transfer coefficient;
K is the total heat-transfer coefficient;
Δi is the vaporization;
P is the pressure;
ρ is the density;
V is the volume;
l is the length;
δ is the thickness;
S is the cross-sectional area;
n is the number of corrugations of sylphon bellows;
A, B are the coefficients of linearized elasticity curve for heat-transfer medium.

Indices

E is the vaporator section;

T	is the transport section;
C	is the condenser section;
V	is the vapor-flow passage;
HP	is the heat pipe;
R	is the reservoir;
e	is the end of sylphon bellows;
av	is the average (for siphon bellows);
0	are the initial parameters;
c	is the conduction;
r	is the radiation.

LITERATURE CITED

1. S. W. Kessler, "Transient thermal impedance of a water heat pipe," ASME Paper No. 71-WA/HT-9 (1971).
2. F. Edelstein and R. J. Hembach, "Design, fabrication, and testing of a variable conductance heat pipe for equipment thermal control," AIAA Paper No. 422 (1971).
3. V. V. Kafarov, Cybernetic Methods in Chemistry and Chemical Technology [in Russian], Khimiya, Moscow (1968).
4. G. N. Dul'nev and É. M. Semyashkin, Heat Transfer in Radio-Electronic Equipment [in Russian], Énergiya, Leningrad (1968).
5. S. S. Kutateladze and V. M. Borishanskii, Heat-Transfer Handbook [in Russian], Gozénergoizdat, Moscow (1969).
6. V. V. Barsukov, L. N. Mishchenko, and G. F. Smirnov, "Limiting characteristics of low-temperature heat pipes," Inzh.-Fiz. Zh., 25, No. 2 (1973).

MAXIMUM HEAT-TRANSFER CAPACITY OF A VERTICAL TWO-PHASE THERMAL SIPHON

M. G. Semena

UDC 536.27:669.214

A survey of the experimental data on the maximum heat-transfer capacity of a two-phase thermal siphon is presented; a physical model that describes many of the experimental data on the heat-transfer limits for thermal siphons is proposed.

A two-phase thermal siphon works with an evaporation–condensation cycle and represents an efficient heat-transfer device that can often compete successfully with other heat exchangers.

The limiting heat flux carried by such a siphon is a major working characteristic; however, at present there is no agreed view on the limit to the heat transfer through a vertical two-phase siphon. This limit may be called the critical heat transfer. Various types of crisis should be distinguished [1] in terms of the physical principles. There is a deterioration in the heat transfer if the layer of liquid at the wall is disrupted by the interaction between the phases (type I crisis). The film of liquid evaporates on account of inadequate supply in a type II crisis. Here we consider the crisis arising from interaction between the phases, which disturbs the countercurrent flow in the two-phase boundary layer. Many of the experimental results are qualitative rather than quantitative.

For example, the drying occurring at the heating surface has been discussed [2, 3] in terms of interaction between the countercurrents of vapor and liquid. A qualitative description of this phenomenon has been given [3], while the relationship given in [2] applies only for the conditions considered in that paper, and it cannot be used, for example, to explain the heat-transfer limit due to instability in the liquid film [4]. In [5],

Kiev Polytechnic Institute. Translated from Inzhenerno-Fizicheskii Zhurnal, Vol. 35, No. 3, pp. 397-403, September, 1978. Original article submitted March 21, 1977.

